ACS APPLIED MATERIALS & INTERFACES

Research Article

www.acsami.org

Liquid-Filled Metal Microcapsules

Marcia W. Patchan, Lance M. Baird, Yo-Rhin Rhim, Erin D. LaBarre, Adam J. Maisano, Ryan M. Deacon, Zhiyong Xia, and Jason J. Benkoski*

Research and Exploratory Development Department, Adpplied Physics Laboratory, The Johns Hopkins University, Laurel, Maryland 20723, United States

ABSTRACT: A moisture-sensitive diisocyanate liquid is microencapsulated within a metal shell measuring less than 2 μm thick and 50 μm in diameter. This mild synthesis takes place through a series aqueous processing steps that occur at or near room temperature. Through a combination of emulsification, interfacial polymerization, and electroless plating, one can microencapsulate moisture- or air-sensitive chemicals within a metal seal. The liquid-filled metal microcapsules promise a number of advantages compared to conventional polymeric microencapsulation, including improved mechanical properties and improved barrier properties to gases and organic molecules.

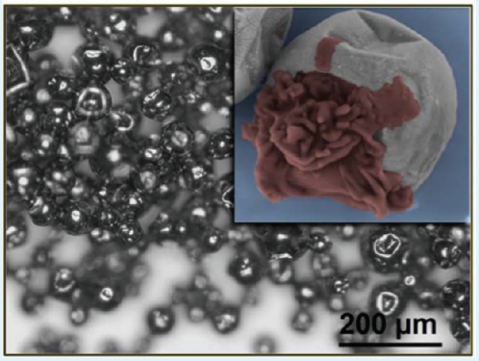

KEYWORDS: *microencapsulation, emulsion, interfacial polymerization, electroless plating*

INTRODUCTION

This study presents a facile method for producing liquid-filled, metal microcapsules in large quantities. Through a combination of emulsification, interfacial polymerization, and electroless metal deposition, we demonstrate successful encapsulation of a water-sensitive chemical—isophorone diisocyanate (IPDI)—within a nickel shell (Figure 1). Liquid-filled microcapsules already find wide use in consumer products including carbonless paper,[1−3] pesticides,[4] and fragrances.[5−7] Current applications are limited, however, to situations where the entrained liquids are not air sensitive or where the outgassing of volatiles can be tolerated. Both limitations stem from the relatively poor barrier properties of polymer membranes.[8] Not only would a metal provide improved protection, but its mechanical, electrical, optical, and magnetic properties could also be exploited for interesting new applications.

A number of research groups have attempted to enhance microcapsules through the addition of inorganic materials into the outer shell. None, to the best of our knowledge, have encapsulated a liquid as a discrete droplet with a continuous metal shell. Competing technologies generally employ a particulate filler in the polymer shell. One such example consists of gold nanowires self-assembled at the oil/water interface of an emulsion.[9] Another approach was to deposit hydrogen-bonded polymer multilayers on a polystyrene colloid, reduce Ag or Pd ions to the corresponding metal, and then dissolve the polystyrene away to leave behind a hollow microcapsule.[10] Other methods for preparing inorganic microcapsules dispense with the use of a polymer matrix.[11] Morishige, et al. demonstrated the synthesis of hollow metal-silicate microcapsules using a water/oil/water emulsion.[12] Also formed without a polymer scaffold were hollow, mesoporous Pd, PdO, RuO_2, and IrO_2 microcapsules.[13]

The few attempts at encapsulating liquids with a continuous metal have not resulted in discrete microcapsules. Rather, these materials have consisted of electrodeposited films with liquid inclusions. In one case, copper films were deposited with organosilica liquid,[14] and in another, water was encapsulated within a nickel film during electrodeposition.[15] Both methods essentially started with liquid-filled polymer microcapsules, and then codeposited the microcapsules along with metal during the electrodeposition process.

A key driver for the development of metal microencapsulation is to improve the shelf life of microencapsulated compounds that react with water or oxygen. The moisture-sensitive compound must have a relatively low reaction rate with water to survive the aqueous emulsification process described here; however, reverse-phase emulsification can overcome these limitations for some compounds.[16] Subsequently encapsulating such liquids within a continuous metal shell rather than a polymer provides a number of advantages, including the potential to hermetically seal a liquid that is water or air sensitive and the ability to prevent outgassing of volatile encapsulants. These capabilities follow from the vastly improved barrier properties of a metal relative to a polymer.[17] Small molecules such as water and oxygen readily permeate most polymers, with typical rates ranging from 0.1 to 10 barrers (2 atm, 35 °C).[8] The relatively rapid diffusion is a function of the large free volume within a polymer, which provides a low

Received: December 30, 2011
Accepted: April 17, 2012
Published: April 17, 2012

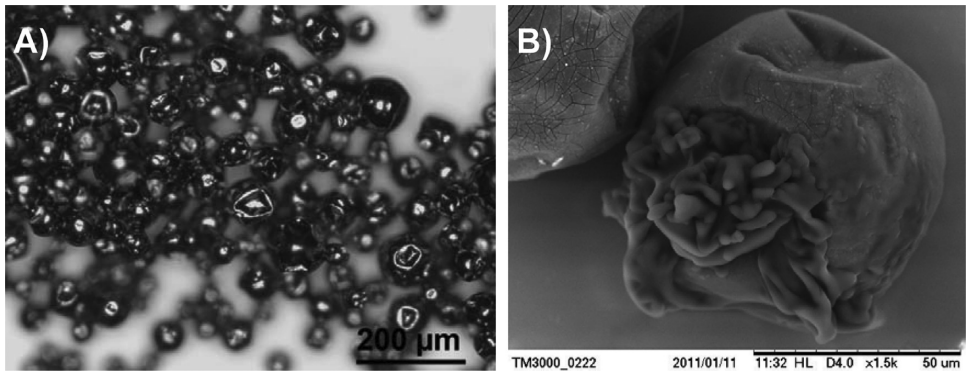

Figure 1. (A) Optical micrograph of Ni-plated microcapsules, and (B) SEM micrograph of Ni microcapsule heated by electron beam to cause rupture.

resistance pathway.[18] Metals, on the other hand, permit diffusion of gas molecules only through interstitial hopping, vacancy diffusion, or grain boundary diffusion of the constituent atoms.[19] For similar reasons, metals also prevent the permeation of small organic molecules. Polymers, in contrast, can permeate even relatively large organic molecules, particularly if they are soluble in the polymer.

Another implication of the metal shell is improved mechanical durability. The Young's modulus of a metal such as nickel is typically about 100 times greater than a glassy polymer.[20] The yield strength and ultimate tensile strength are at least an order of magnitude greater as well. To put these terms into perspective, a closed-cell foam consisting of hollow spheres will have an elastic modulus (E_f) equal to[21]

$$E_f = E_s C_2 \left(\frac{\rho_f}{\rho_s}\right) = E_s C_2 \left(\frac{\phi\pi}{6}\right) \quad (1)$$

where E_s is the Young's modulus of the solid, C_2 is a constant ≈ 1 in this limit, ρ_f is the density of the foam, ρ_s is the density of the solid, and ϕ is the fraction of solid in the hollow sphere. This equation predicts that a hollow nickel sphere consisting of just two percent metal will have the same stiffness as solid polyurethane. One could then conceivably incorporate metal-coated microcapsules into a polymer composite with a negligible loss in mechanical properties.

A particularly intriguing application for metallic microcapsules is self-healing polymers. Sottos and White have demonstrated that monomer-filled microcapsules release their contents into a growing crack where they polymerize, repairing the crack.[22−28] Much like the microcapsules described in the current paper, Yang and co-workers synthesized IPDI-filled microcapsules, introducing the possibility of a one-part, catalyst-free self-healing system.[28] The key difference is the addition of a hard, metallic shell, which would be expected to improve the mechanical properties of the microcapsule composite and the shelf life of the entrained diisocyanate.

The final advantages of a metal shell are that the optical, electrical, thermal, and magnetic properties differ so much from a polymer. These differences alone offer interesting possibilities with respect to the appearance, concealment, electrical conduction, thermal conduction, magnetic separation, or possibly even triggered release. Taken together, the many advantageous properties of a metal shell underlie the importance of developing a facile method for synthesizing metal-coated microcapsules. Herein we report the step-by-step fabrication and subsequent characterization of 36 μm nickel microcapsules filled with IPDI. Although microcapsules were synthesized with a wide variety of diameters, compositions, and shell thicknesses, we focus our attention on a single formulation for clarity.

EXPERIMENTAL SECTION

Reagents. All reagents were purchased from Sigma Aldrich and used without further purification unless otherwise noted. Isophorone diisocyanate (CAS [4098−71−9]), Poly[(phenyl isocyanate)-co-formaldehyde] (CAS [9016−87−9]; $M_n \approx 400$), Poly(ethylenimine) 50% (aq) (CAS [9002−98−6]; $M_n \approx 60\,000$), Poly(acrylic acid) 35% (aq) ($M_w \approx 100\,000$), gum arabic (CAS [9000−01−5]), nickel(II) sulfate hexahydrate (CAS [10101−97−0]), sodium hypophosphite (CAS [7681−53−0]), DL-lactic acid (CAS [50−21−5]), DL-malic acid (CAS [6915−15−7]), Tergitol NP-9 (CAS [9016−45−9]), sodium acetate (CAS [127−09−3]), ammonia 4.6N (aq) (CAS [1336−21−6]), diethylenetriamine (CAS [111−40−0]), tin(II) chloride (CAS [7772−99−8]), palladium(II) chloride (CAS [7647−10−1]), and hydrochloric acid (CAS [7647−01−1]).

Scheme 1. Reaction Scheme for the Synthesis of Liquid-Filled Metal Microcapsules

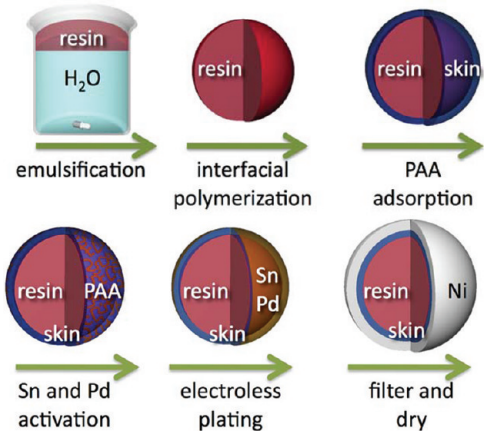

Microcapsule Synthesis. The synthesis of liquid-filled, metal microcapsules is outlined in Scheme 1. Oil-in-water emulsification accompanied by interfacial polymerization produced spherical microcapsules with a liquid interior and thin polymer shell. An IKA overhead stirrer (Model # 2600001) vortexed the solution. The oil phase was prepared from an 85:15 (w/w) mixture of two isocyanate-functionalized monomers: isophorone diisocyanate (IPDI) and poly[(phenyl isocyanate)-co-formaldyhde] (PPI). The aqueous phase

consisted of a 5% (w/v) aqueous gum arabic solution. The cross-linker solution contained a mixture of the water-soluble cross-linkers diethylenetriamine (DETA) and polyethylenimine (PEI) at 5% (w/v) each in the 5% (w/v) aqueous gum arabic. Twenty g of monomer mixture was added to 75 mL of a 5% (w/v) aqueous gum arabic solution and stirred at 2000 rpm using the IKA stirrer. Shortly thereafter, 20 g of cross-linker solution was added while the mixture was stirring. Stirring continued for 3 h. Following stirring, the mixture was allowed to react for 3 days before purifying. The supernatant liquid was decanted and the microcapsules were washed 3x with Milli-Q water (18.2 MΩ). The reaction yielded 20 g of microcapsules.

Electroless Deposition. Microcapsules (20 g) were washed once with 100 mL of a 100 mM PBS buffer pH 7.4, and then placed into 100 mL of a 2% (w/v) poly(acrylic acid) solution (aq) in 100 mM PBS buffer pH 7.4 and allowed to stir for 10 min. These microcapsules were decanted and washed once with the 100 mM PBS buffer and then twice with Milli-Q water. The microcapsules were then placed into 100 mL of an acidic $SnCl_2$ solution (10 g/L $SnCl_2$ and 5 mL/L HCl) and allowed to stir for 10 min. The microcapsules were decanted and washed 3× with Milli-Q water. Microcapsules were then immersed in an acidic $PdCl_2$ (aq) solution (0.5 g/L $PdCl_2$ and 4 mL/L HCl) for 2 min. These microcapsules were then decanted and washed 3x with Milli-Q water. The activated microcapsules were placed into an electroless plating solution containing: 29.8 g/L nickel sulfate hexahydrate, 100 g/L sodium hypophosphite, 21 mL/L DL-lactic acid, 4 g/L DL-malic acid, 1 mg/L Tergitol NP-9, and 8.5 g/L sodium acetate. 4.6 N ammonia (aq) was used to adjust the plating solution's pH to ~4.7−4.8. The solution was heated to 60 °C using a Corning hot plate (model # PC-400D) and allowed to plate for 1 h. After plating, the microcapsules were washed and filtered 3× with Milli-Q water. The microcapsules were then lyophilized to remove any residual water.

Microcapsule Size Analysis. All images were obtained with an Olympus optical microscope (model # BX60MF5) and a Leica DFC306 FX digital camera. Quantitative image analysis of the sphere size distribution was performed using ImageJ image analysis software.

Extent of Polymerization. Thermogravimetric Analysis (TGA) determined the weight fraction of polymer in the microcapsules. A TA Instruments Q5000 TGA ramped the temperature at 10 °C/min under nitrogen gas from 25 to 500 °C. The fully cured polymer decomposed at approximately 359 °C, whereas the pure resin decomposed around 231 °C. The weight fraction of liquid in the microcapsules could therefore be calculated from the plateau in weight loss at 340 °C, after the completion of the liquid decomposition and just prior to the onset of polymer decomposition.

Differential Scanning Calorimetry Measurements. The glass transition temperature was measured using differential scanning calorimetry (DSC) using a Mettler-Toledo Differential Scanning Calorimeter with FRS5 sensor. The measurements were taken from −70 to 100 °C at a ramp rate of 20 °C/min. The sample was sealed in 40 μL aluminum hermetic pan with a liquid nitrogen cooling source.

Metal Thickness Measurements. The thickness of the metal coating was determined through SEM images of the cross sectioned microcapsules. Microcapsules were immobilized into a cured epoxy resin and microtomed to reveal their cross-sections. The microtomed samples were imaged via a Hitachi SEM model S4700.

Metal Coating Composition. The chemical composition of the metal coating was analyzed using a Hitachi S4700 scanning electron microscope (SEM), with an EDAX energy dispersive X-ray spectroscopy (EDS) system. EDS analysis was conducted at 20 kV on Ni-coated microcapsules that were dispersed on a glass slide.

RESULTS AND DISCUSSION

Microcapsule Size. The first step of microcapsule synthesis is the emulsification of an oily mixture of isocyanate monomers in water. Factors that influence the size of the microcapsules include the blade geometry, blade hydrodynamics, viscosity, interfacial tension, shear rate, and temperature.[11] By holding the reagent concentrations and temperature constant, the size of the microcapsules could be controlled by changing the spin speed of the overhead stirrer. The stirring rate was varied from 500 to 2000 rpm to determine the relationship with particle size distribution Figure 2 displays the average microcapsule

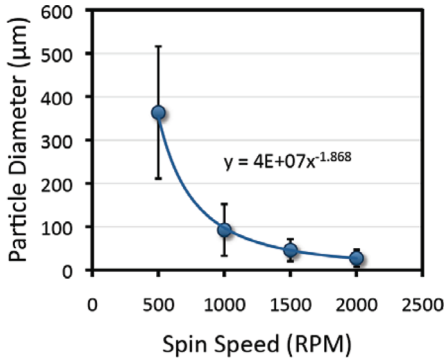

Figure 2. Average diameter size as a function of mixing speed. The error bars represent the standard deviation.

diameter as a function of mixing speed. In all, metal microcapsules have been synthesized ranging in size from 10 to 500 μm. Since purification was performed by sedimentation and decanting, larger microcapsules could be produced more easily and in higher yield. No practical limits were observed beyond the fact that the smallest microcapsules took longer to purify and carried a smaller payload. Nevertheless, smaller microcapsules are more attractive for applications that require fine dispersions. A stir rate of 2000 rpm yielded an average diameter of 36 ± 17 μm, which was used for all microcapsule synthesis in this study.

Polymer Skin Thickness. The second step of microencapsulation is to form a solid polymer skin around the oily droplets through an interfacial polymerization. Though they react with water, isocyanates more readily polymerize with amine-functionalized cross-linkers that can be added to the aqueous phase.[29] As the polymerization proceeds, the increasing molecular weight causes the polymer to become less soluble in the monomer and segregate to the interface. The interfacial buildup then decreases the permeability of cross-linker and water into the core, arresting further reaction.

Shelf life considerations require the skin layer to be as impermeable as possible. Pilot experiments showed that porous or damaged polymer skin layers lead to poor longevity or an inability to survive electroless plating. Such skin layers were thin and viscoelastic. Above a critical extent of polymerization, the skin layer underwent a rubbery to glassy transition, which was accompanied by vastly improved barrier properties. It could be readily identified by the brittle fracture mechanism displayed by the microcapsules under applied pressure. This behavior was used as a quick method to determine whether the microcapsules could withstand electroless plating (Figure 3).

As shown by Fox and Flory,[30] the glass transition temperature (T_g) increases with increasing molecular weight (M_n).

$$T_g = T_g^{\infty} - \frac{K}{M_n} \tag{2}$$

where T_g^{∞} is the glass transition temperature at infinite molecular weight, and K is a constant. T_g^{∞} for fully cured microcapsules was measured to be 58 °C by differential scanning calorimetry. Equation 2 shows that T_g increases with

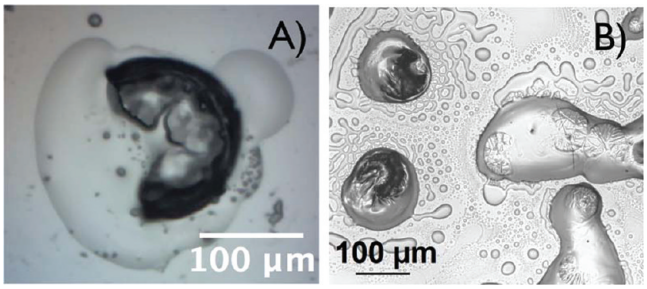

Figure 3. (A) Optical microscopy image detailing the "egg-shell" structure of optimally formed microcapsules. (B) Set of suboptimal microcapsules, where the remains of several broken polymer shells merely float on top of the released IPDI. Prior to rupture, the polymer stretches many times its own diameter, rather than cracking.

molecular weight until it reaches its terminal value of 58 °C. In practical terms, the polymer skin layer becomes glassy when M_n is sufficiently high to drive T_g above room temperature. Thermogravimetric analysis (TGA) indicated that this transition occurred at about the same time that the solid fraction reached 0.2 (w/w) for the microcapsule (Figure 4A). A typical TGA trace is shown in Figure 4B. This extent of polymerization was used for all microcapsules in this study.

To calculate the polymer skin thickness from the volume fraction of liquid, simply calculate volume of liquid relative to the volume of the microcapsule, then take the polymer skin thickness as the difference between the radius of the microcapsule and the radius of the equivalent liquid sphere. For 80% liquid, a 37 μm microcapsule will have a 1.3 μm thick polymer shell according to this calculation. This value assumes that polymerization occurred only at the interface, which was true for reactions performed at room temperature. Yang, et al. showed for similar IPDI microcapsules that the polymer skin thickness was proportional to the diameter and that the weight fraction of polymer was fixed for a given set of reaction conditions.[28]

Internal Curing. By choosing an appropriate reaction time, a glassy polymer skin layer with good barrier properties can be produced regardless of monomer composition, cross-linker composition, or temperature; however, a competing internal polymerization causes large differences in the quality of the encapsulated resin. Emblematic of the internal polymerization is the formation of spherical polyurea precipitates (Figure 5). These precipitates form when water and cross-linker diffuse beyond the polymer membrane at the interface.[31]

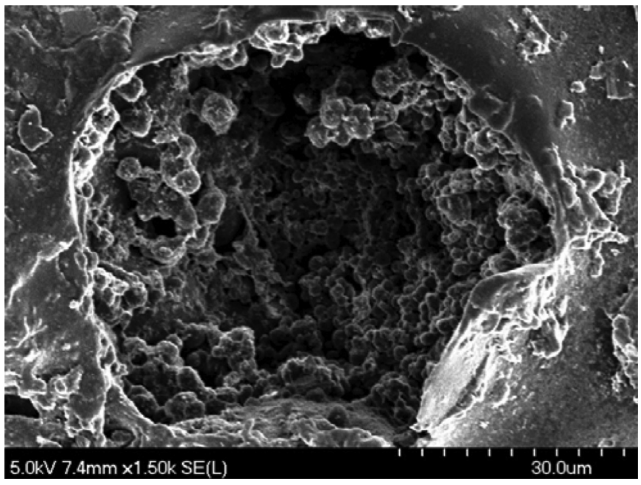

Figure 5. SEM micrograph showing the cross-section of a microcapsule produced at 70 °C. The spherical structures within the core of the microcapsule are polymerized IPDI that precipitate from the monomer and attach to the inside of the microcapsule until curing completes.

The extent of this internal curing is a question of kinetics. To prevent colloid formation, the interfacial polymerization must occur much faster than the internal polymerization. A series of microcapsules were therefore synthesized under varying conditions to determine how they affected these two polymerization rates. Holding the extent of polymerization constant at 0.2, the amount of precipitate was compared using an optical microscope as a function of isocyanate monomer reactivity (IPDI versus toluenediisocyanate), isocyanate monomer functionality (toluenediisocyanate versus PPI), cross-linker reactivity (1,4-butanediol versus ethylenediamine), cross-linker functionality (ethylene diamine, DETA, and PEI), cross-linker concentration (1–20% w/v), and temperature (25–70 °C).

Most of the above combinations exhibited internal curing, but the strongest effects arose from temperature (Figure 6). At 25 °C, an impermeable skin layer would thicken slowly but

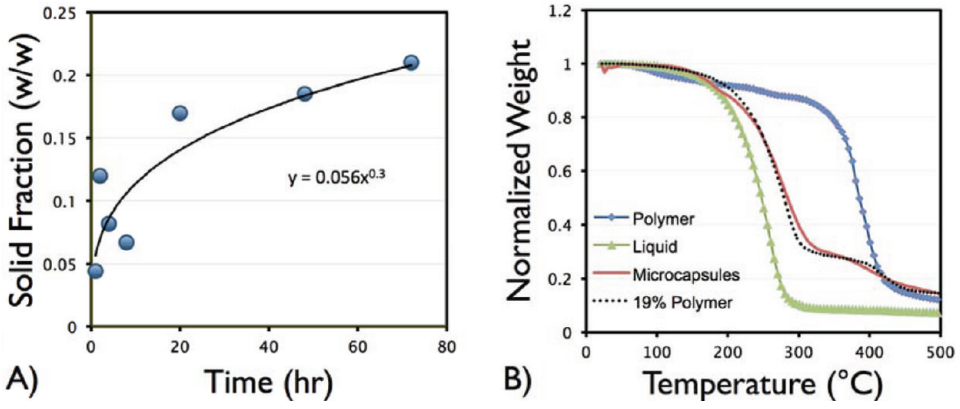

Figure 4. (A) TGA data of the liquid filled microcapsules on a Perkin-Elmer TGA. The solid fraction was determined by comparing the relative mass loss at 231 °C due to the liquid to the loss at 359 °C due to the solid. Above a solid fraction of 0.2, the polymer skin layer exhibited brittle, glassy behavior. (B) Representative TGA trace showing the mass loss of the uncured monomer mixture, the fully cured polymer, and a representative microcapsule sample. The dotted line shows a fit to the microcapsule trace formed by linear mixing of the polymer and liquid traces.

dx.doi.org/10.1021/am201861j | ACS Appl. Mater. Interfaces 2012, 4, 2406–2412

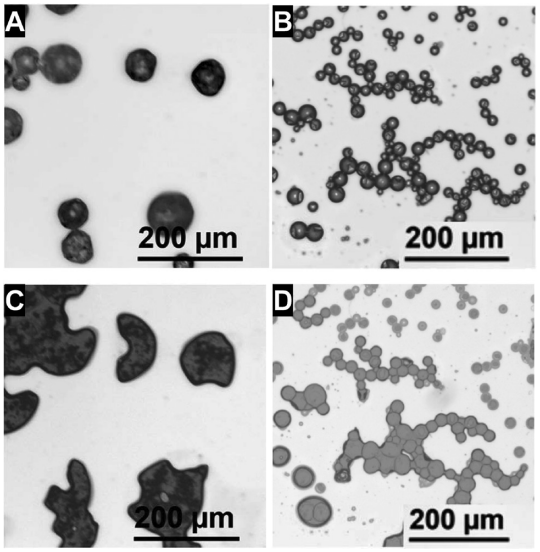

Figure 6. Optical micrographs comparing the degree of internal curing of microcapsules formed at (A) 70 and (B) 25 °C. (C) Microcapsules formed at 70 °C have a speckled appearance when squashed underneath a coverslip. These polymer precipitates could be seen flowing out of the microcapsules along with the liquid with continued depression of the coverslip. (D) Microcapsules formed at 25 °C are completely transparent when squashed underneath a coverslip.

without the accompanying precipitate. At 70 °C, the internal polymerization prevailed. This abrupt change appears to be correlated to T_g. Because the polymer skin layer remains rubbery at 70 °C, it has poor barrier properties and facilitates internal curing almost regardless of skin thickness.

In contrast to these observations, Li and co-workers had shown that interfacial polymerization for a comparable isocyanate system produced dense barrier layers at elevated temperatures, and porous membranes at low temperatures.[32] Although these results appear to contradict the current data, their study did not investigate high molecular weight cross-linkers such as PEI. Room temperature synthesis using diethylenetrieamine, ethylenediamine, or butanediol may very well form denser polymers at higher temperatures, but the microcapsules formed by PEI at room temperature boasted the longest shelf life (>9 months) and lowest internal polymerization (~ 0%) of all samples studied. Shelf life was routinely measured for all samples by taking small aliquots periodically and crushing them to release entrained liquid. Sample-to-sample variability precludes a detailed analysis except to note that microcapsules formed without PEI or at high temperatures generally solidified completely within two months. Microcapsules formed at room temperature have routinely lasted 6–9 months with no noticeable loss in liquid fraction as of this writing.

pH Sensitivity. The thicker, glassy shell appears to play a second function. Additional experiments revealed that alkaline plating baths etch the polymer skin layer. A thicker polymer skin may therefore protect the microcapsules against etching during the electroless plating step. Fresh microcapsules placed in Ni plating baths with a pH of 4.7, 10, and 12.4 are compared in Figure 7. Although the control samples and acid bath samples remain transparent, the basic plating baths both result in opaque microcapsules after only 1 h. The opaque appearance results from spherical polymer precipitates described in the previous section. The precipitates suggest that the basic solution etches the polymer skin layer, allows water to infiltrate the microcapsule, and then drives unwanted internal curing.

Under normal circumstances, the metal might otherwise be expected to protect the polyurea skin against hydrolysis. However, the frequent occurrence of complete curing in a basic plating bath suggests that etching may occur at a fast enough rate to compete with the plating reaction at high pH. Because the amount of etching is negligible at low pH, acidic nickel plating baths were used in this study.

Ni:Zn Metal Shell. Coating polymers with metal via electroless deposition has in the past been challenging.[33] The biggest obstacle is the need for a harsh acidic etching step to activate the polymer's surface for palladium adsorption. Etching has proven to destroy the microcapsules produced in this research. Since oxidation essentially produces a surface rich in carboxylic acids, the oxidation step was replaced with the deposition of poly(acrylic acid) (PAA). PAA, already in a high oxidation state, readily deposits on the excess amine groups left over from the polyurea interfacial polymerization. This process is a variant of the widely used layer-by-layer polyelectrolyte deposition technique.[34−36] The resulting surface is smoother and more chemically uniform than a comparable oxidized

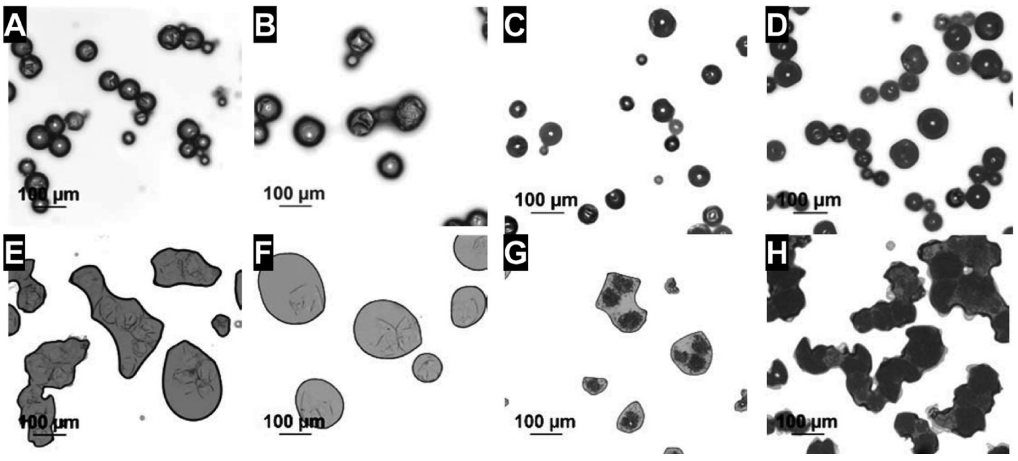

Figure 7. Optical micrographs of microcapsules exposed to plating baths for 1 h. (A) Control with no plating bath exposure, (B) pH 4.7, (C) pH 10, (D) pH 12.4. (E–H) Same as above but after squashing with a coverslip to reveal internal curing.

surface, and yet it strengthens the polymer skin layer instead of etching through it.

After inverting the surface charge, Sn^{2+} readily deposited on the PAA-coated surface (Scheme 1). The Sn^{2+} then reduced Pd^{2+} from solution to create Sn^{4+} and Pd^0. Metallic Pd would then catalyze the subsequent Ni plating reaction, where sodium hypophosphite would reduce Ni^{2+} to metallic Ni^0. Without Sn/Pd activation, the Ni films would not adhere to the polymer surface. In many cases, the plating reaction would not occur at all, or plating would occur preferentially on the glass beaker. Efficient catalysis of the plating reaction is critical for maintaining high yields in the current application due to the relative fragility of the liquid-filled polymer microcapsules. Better catalysis makes it possible to plate under milder conditions. However, others have shown that Pd^0 colloids complexed with poor π-acceptor ligands bind directly to surface amine sites, potentially obviating the need for PAA deposition in this system.[37] Also possible is the adsorption of Cu^{2+}, Ni^{2+}, or Co^{2+} on the PAA coating followed by reduction to create a cheaper, more environmentally friendly catalyst.[38−40]

A standard Ni−P electroless plating solution, which employs sodium hypophosphite to reduce the nickel ion, was used to coat the PAA-activated surfaces.[41,42] Figures 1 and 8A show

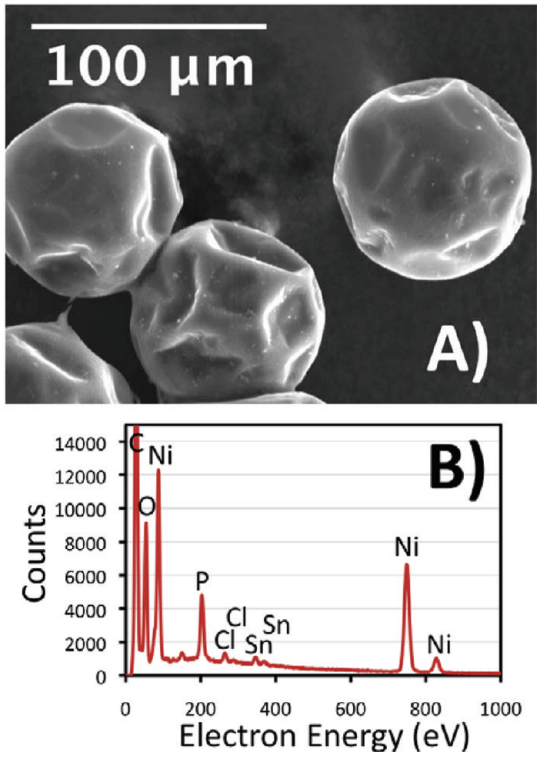

Figure 8. (A) SEM micrograph and (B) the accompanying EDS spectrum taken at 20 kV, showing the presence of nickel.

that liquid-filled, metal microcapsules could be produced by this process in high yield. Yields typically exceeded 90%. The only losses came during the decanting steps, and these losses could be reduced even further by centrifuging the microcapsules into a pellet rather than using sedimentation. Using a centrifugal acceleration of 10 *g* for 2 min achieved the right balance between forming a solid pellet and being able to redisperse the microcapsules with gentle agitation. EDS analysis (Figure 8B) confirmed the presence of nickel on the microcapsules. Measured by SEM cross sectional analysis of the microcapsules (Figure 9), the thickness metallic layer was approximately 1.4

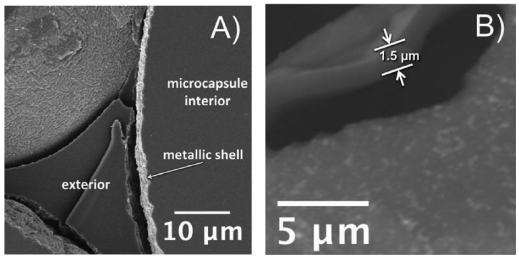

Figure 9. (A) SEM cross-section of a fully cured microcapsule. The metallic shell wall was determined to be 1.4 μm in thickness after 1 h of electroless plating at 60 °C. B) SEM of a cracked microcapsule after the liquid has been removed. This unplated microcapsule reveals a polymer skin thickness of 1.5 μm, which is the thickness that would be calculated for a 42 μm diameter microcapsule with a solids fraction of 0.2.

μm thick after 1 h of plating. The smooth, unbroken Ni films provided excellent barrier coatings, as liquid IPDI was recovered from broken microcapsules that had been stored under ambient conditions for 9 months.

A common challenge in electroless plating in aqueous solution is that H_2 evolution can compete with metal deposition. H_2 gas bubbles can adhere to the surface, causing pitting and lowering product yields. Figure 10A shows an

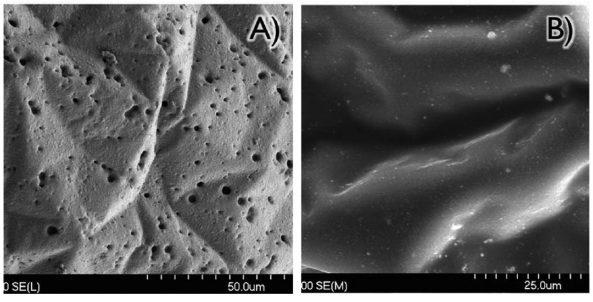

Figure 10. (A) SEM of metal microcapsule that was plated without the use of surfactant. Pitting occurs because H_2 generated during the plating reaction adheres to the surface and prevents metal deposition at that location. (B) Smooth nickel films can be produced by adding 1 mg/L Tergitol NP-9 surfactant to the plating bath.

example of pitting using this process. However, pitting can be completely suppressed through the addition of 1 mg/L Tergitol NP-9 to the plating solution. Tergitol NP-9 lowers the surface tension of the gas bubbles, reducing adhesion with the microcapsules during plating. Figure 10B shows an example of the smooth, defect-free plating that results from the use of surfactant. The surfactant provided an additional benefit: it helped maintain dispersal of the microcapsules during the plating process. Between the churn of the solution caused by the hydrogen evolution and the surfactant stabilization of the dispersion, agglomerates were rarely observed. When agglomerates did form, they mostly consisted of two or three particles.

An unintended consequence of this mild electroless plating procedure is that virtually any film deposited by polyelectrolyte multilayer deposition can be subsequently coated with a thin metal film. Hendricks and Lee previously demonstrated the versatility of this method for depositing both nickel and copper

on a variety of substrates and in a variety of patterns.[43,44] Nickel was used in the current study, but copper, nickel–zinc alloys, and cobalt coatings are also possible. The combination of these two bottom-up fabrication techniques could lead to control of the composition down to the nanoscale. Essentially any capability that has been demonstrated for polyelectrolyte multilayers—thickness control, patterning, composites, membrane formation—may now be further enhanced by the ability to include metal layers with the same degree of dimensional control.[34,35,45]

CONCLUSION

We have successfully demonstrated the encapsulation of a moisture sensitive liquid within a metal shell. Measuring less than 50 μm in diameter, each metal microcapsule protects its contents, and has shown the ability to preserve a moisture-curable polyurethane precursor for at least 9 months as of this writing. Since the synthesis steps are based entirely on industrial processes, this technique should scale easily to large batch sizes. Finally, the ease with which a metal may be applied to a negatively charged polymer from aqueous solution has further implications in the fabrication of novel metal–polymer composites and metamaterials with unique mechanical, optical, magnetic, and electrical properties.

AUTHOR INFORMATION

Corresponding Author

*E-mail: jason.benkoski@jhuapl.edu.

Notes

The authors declare no competing financial interest.

ACKNOWLEDGMENTS

This research was funded by the Office of Naval Research under grant # N00014-09-1-0383. Funding for the writing of this paper was made possible through a Janney fellowship from the Johns Hopkins University Applied Physics Laboratory. We would also like to thank Dr. Rengaswamy Srinivasan, Dr. Tracy Terry, and Dr. Andrew Mason for their helpful discussions.

REFERENCES

(1) Bielinski, J. *Metalloberflaeche* **1984**, *38*, 1.
(2) White, M. A. *J. Chem. Educ.* **1998**, *75*, 1119.
(3) Drechsler, G. W. *Coating* **1986**, *9*, 310.
(4) Stadelhofer, J. W.; Zellerhoff, R. B. *Chem. Ind. (London)* **1989**, *7*, 208.
(5) Scher, H. B.; Rodson, M.; Lee, K.-S. *Pestic. Sci.* **1998**, *54*, 394.
(6) Nelson, G. *Intl. J. Pharm.* **2002**, *242*, 55.
(7) Kraft, P.; Bajgrowicz, J. A.; Denis, C.; Fráter, G. *Angew. Chem., Int. Ed.* **2000**, *39*, 2980.
(8) Brannon-Peppas, L. *ACS Symp. Series* **1993**, *520*, 42.
(9) Patra, D.; Malvankar, N.; Chin, E.; Tuominen, M.; Gu, Z.; Rotello, V. M. *Small* **2010**, *6*, 1402.
(10) Lee, D.; Rubner, M. F.; Cohen, R. E. *Chem. Mater.* **2005**, *17*, 1099.
(11) Wang, L.-Y.; Tsai, P.-S.; Yang, Y.-M. *J. Microencapsulation* **2006**, *23*, 3.
(12) Morishige, I.; Toorisaka, E.; Hirata, M.; Ohtake, T.; Hano, T. *J. Microencapsulation* **2005**, *22*, 291.
(13) Ren, N.; Dong, A.-G.; Cai, W.-B.; Zhang, Y.-H.; Yang, W.-L.; Huo, S.-J.; Chen, Y.; Xie, S.-H.; Gao, Z.; Tang, Y. *J. Mater. Chem.* **2004**, *14*, 3548.
(14) Liqun, Z.; Wei, Z.; Feng, L.; He, Y. *J. Mater. Sci.* **2004**, *39*, 495.
(15) Kentepozidou, A.; Kiparissides, C.; Kotzia, F.; Kollia, C.; Spyrellis, N. *J. Mater. Sci.* **1996**, *31*, 1175.
(16) McIlroy, D. A.; Blaiszik, B. J.; Caruso, M. M.; White, S. R.; Moore, J. S.; Sottos, N. R. *Macromolecules* **2010**, *43*, 1855.
(17) Prins, W.; Hermans, J. J. *J. Phys. Chem.* **1959**, *63*, 716.
(18) Wang, Z. F.; Wang, B.; Qi, N.; Zhang, H. F.; Zhang, L. Q. *Polymer* **2005**, *46*, 719.
(19) Porter, D. A.; Easterling, K. E., *Phase Transformations in Metals and Alloys*, 2nd ed.; Chapman & Hall: London, 1993; pp 60–106.
(20) Hertzberg, R. W. *Deformation and Fracture Mechanics of Engineering Materials*; John Wiley & Sons: New York, 1996; p 7.
(21) Clancy, R. B.; Cochran, J. K.; Sanders, T. H. *Mater. Res. Soc. Symp. Proc.* **1995**, *372*, 5.
(22) Brown, E. N.; White, S. R.; Sottos, N. R. *J. Mater. Sci.* **2004**, *39*, 1703.
(23) Rule, J. D.; Brown, E. N.; Sottos, N. R.; White, S. R.; Moore, J. S. *Adv. Mater.* **2005**, *17*, 205.
(24) Jones, A. S.; Rule, J. D.; Moore, J. S.; Sottos, N. R.; White, S. R. *J. R. Soc. Interface* **2007**, *4*, 395.
(25) Cho, S. H.; Andersson, H. C.; White, S. R.; Sottos, N. R.; Braun, P. V. *Adv. Mater.* **2006**, *18*, 997.
(26) Brown, E. N.; Kessler, M. R.; Sottos, N. R.; White, S. R. *J. Microencapsulation* **2003**, *20*, 719.
(27) Brown, E. N.; Kessler, M. R.; Sottos, N. R. *J. Mater. Sci.* **2006**, *41*, 6266.
(28) Yang, J.; Keller, M. W.; Moore, J. S.; White, S. R.; Sottos, N. R. *Macromolecules* **2008**, *41*, 9650.
(29) Lu, Q.-W.; Hoye, T. R.; Macosko, C. W. *J. Polym. Sci., Part A: Polym. Chem.* **2002**, *40*, 2310.
(30) Fox, T. G.; Flory, P. J. *J. Appl. Phys.* **1950**, *21*, 581.
(31) Note that the data in Figure 4 does not include any samples that exhibited internal polymerization. Samples such as the one depicted in Figure 5 had the requisite glassy polymer skin layer for electroless plating, but the presence of polymer inside the microcapsule probably indicates that the overall extent of polymerization was higher than 0.2.
(32) Li, J.; Hitchcock, H. P.; Stover, H.; Shirley, I. *Macromolecules* **2009**, *42*, 2428–2432.
(33) Sipaut, C. S.; Mohamad Ibrahim, M. N.; Izat, M. E. *J. Appl. Polym. Sci.* **2007**, *103*, 1554.
(34) Decher, G. *Science* **1997**, *277*, 1232.
(35) Decher, G.; Hong, J.-D. *Makromol. Chem., Macromol. Symp.* **1991**, *46*, 321–327.
(36) Hammond, P. T.; Whitesides, G. M. *Macromolecules* **1995**, *28*, 7569.
(37) Zabetakis, D.; Dressick, W. J. *ACS Appl. Mater. Interfaces* **2009**, *1*, 4.
(38) Matsumara, Y.; Enomoto, Y.; Sugiyama, M.; Akamatsu, K.; Nawafune, H. *J. Mater. Chem.* **2008**, *18*, 5078.
(39) Garcia, T.; Berthelot, P.; Viel, A.; Mesange, P.; Jégou, F.; Nekelson, S.; Roussel, S. P. *ACS Appl. Mater. Interfaces* **2010**, *2*, 1177.
(40) Chen, S.-T.; Chen, G.-S. *Langmuir* **2011**, *27*, 12143.
(41) Lyunyatskas, M.; Tarozaite, R.; Gyanutene, I.; Lyakonis, Yu. *Zh. Prikl. Khim.* **1978**, *51*, 1797.
(42) Bielinski, J.; Goldon, A.; Socko, B.; Bielinska, A. *Metalloberflaeche* **1983**, *37*, 300.
(43) Hendricks, T. R.; Lee, I. *Thin Solid Films* **2006**, *515*, 2347.
(44) Hendricks, T. R.; Dams, E. E.; Wensing, S. T.; Lee, I. *Langmuir* **2007**, *23*, 7404.
(45) Park, J. Y.; Paul, D. R. *J. Membr. Sci.* **1997**, *125*, 23.